Articles

Electron-Transfer Events Leading to Reconstitution of Oxygen-Evolution Activity in Manganese-Depleted Photosystem II Membranes[†]

Anne-Frances Miller[‡] and Gary W. Brudvig*

Department of Chemistry, Yale University, New Haven, Connecticut 06511

Received July 6, 1989; Revised Manuscript Received October 9, 1989

ABSTRACT: O_2-evolution activity and the Mn complex can be reconstituted in photosystem II by a process called photoactivation. We have studied the elementary steps in photoactivation by using electron paramagnetic resonance spectroscopy to probe electron transport in Mn-depleted photosystem II membranes. The electron donation reactions in Mn-depleted photosystem II were found to be identical with those in untreated photosystem II, except that electron donation from the Mn complex was absent and could be replaced by slower electron donation from exogenous Mn^{2+}. Mn^{2+} photooxidation by Mn-depleted photosystem II membranes correlates with reconstitution of O_2-evolution activity. However, photooxidation of Mn^{2+} occurs in competition with photooxidation of the tyrosine residue Y_D, and cytochrome b-559. Thus, these two species are excluded from direct participation in the initial steps in the assembly of the Mn complex. Because photooxidation of Mn^{2+} is slower than photooxidation of the competing electron donors, cytochrome b-559 and chlorophyll, as well as recombination of the charge-separated states chlorophyll$^+Q_A^-$ or $Y_Z^+Q_A^-$, these other reactions dominate in a single photochemical turnover reaction. This provides a molecular basis for both the low yield and low quantum yield of photoactivation. The first photochemical step in the assembly of the Mn complex results in photooxidation of one Mn^{2+} ion. Therefore, the first intermediate in assembly of the Mn complex contains Mn^{3+}. On the basis of these results and previous kinetic studies [Miller, A.-F., & Brudvig, G. W. (1989) *Biochemistry 28*, 8181], we conclude that the second intermediate of Mn complex assembly contains $Mn^{2+}Mn^{3+}$, which is photooxidized to Mn^{3+}_2.

O xygen-evolution activity is acquired or restored in Mn-depleted photosystem II by a process called photoactivation [for review see Tamura and Cheniae (1989)]. Photoactivation consists of Mn photoligation, to assemble the Mn complex, and binding of Ca^{2+}. Although several models have been proposed, the structure of the Mn complex remains unknown, as does the mechanism of Mn complex assembly. A better understanding of the steps by which the Mn complex is assembled would contribute important insight into the nature of the Mn complex. To this end, we have used EPR[1] spectroscopy to observe the species involved in electron transport associated with Mn photoligation.

Although Mn photoligation and O_2 evolution must be mediated by many of the same components of photosystem II, there are some important differences between the two. O_2 evolution proceeds with a high quantum yield, approaching 1, whereas the quantum yield of photoactivation has been calculated to be on the order of only 0.01 (Cheniae & Martin, 1971). Furthermore, photoactivation only occurs in approximately 50% of photosystem II centers with the remaining centers being damaged by competing inactivation reactions. Nonetheless, a complete picture of electron transfer in photosystem II should be able to explain the characteristics of both Mn photoligation and O_2 evolution.

Studies of electron donation in Mn-depleted photosystem II membranes and chloroplasts indicate that Y_D, Y_Z, and cytochrome b-559 remain photochemically active (Babcock & Sauer, 1975; Boussac & Etienne, 1982; Thompson et al., 1989). Thus, although roles in O_2 evolution or protection against photoinhibition have been proposed for several of these cofactors (Thompson & Brudvig, 1988), the possibility remains that some may have essential roles in Mn photoligation.

Cytochrome b-559 and Y_D, in particular, are attractive candidates for roles in Mn photoligation. The correlation between the appearance of high-potential cytochrome b-559 and the appearance of O_2-evolution activity during leaf greening (Plesničar & Bendal, 1973) has suggested a role for cytochrome b-559 in Mn photoligation. Indeed, the reduction potential of high-potential cytochrome b-559 may be sufficiently high to oxidize bound Mn^{2+} to Mn^{3+}. Consideration of the photochemical redox activity of this cytochrome led Cramer et al. (1986) to propose that it might play a role in photoactivation.

No definite role for the tyrosine moiety, Y_D, has been found in O_2 evolution yet. However, experiments by Styring and

---

[1] Abbreviations: Chl, chlorophyll; Y_D, tyrosine electron donor in photosystem II that gives rise to EPR signal II$_{slow}$ when oxidized; DCBQ, 2,5-dichloro-*p*-benzoquinone; DCMU, 3-(3,4-dichlorophenyl)-1,1-dimethylurea; EPR, electron paramagnetic resonance; kDa, kilodalton; MES, 2-(*N*-morpholino)ethanesulfonic acid; P680, primary electron donor in photosystem II; PAGE, polyacrylamide gel electrophoresis; SDS, sodium dodecyl sulfate; Tris, tris(hydroxymethyl)aminomethane; Y_Z, tyrosine electron donor that mediates electron transfer from the Mn complex to P680$^+$.

Scheme I: Electron Donation in O_2-Evolving Photosystem II Membranes[a]
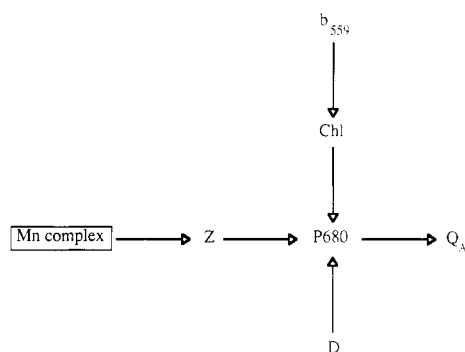
[a] b_{559} stands for cytochrome b-559. All electron donation reactions are reversible except $b_{559} \rightarrow$ Chl.

Rutherford (1987), indicating that Y_D^+ oxidizes the S_0 state of the Mn complex to the S_1 state, suggest that Y_D might be able to participate in oxidizing Mn^{2+} as part of Mn photoligation.

In contrast to the events involved in Mn photoligation, electron donation events involved in O_2 evolution are understood in considerable detail [reviewed in Thompson et al. (1988)]. The primary electron donor of photosystem II, P680, is oxidized transiently in every charge separation and rapidly rereduced by several competing electron donors, Y_Z, Chl, Y_D, cytochrome b-559, and the Mn complex, depicted in Scheme I. Under physiological conditions, photooxidation of the Mn complex via Y_Z is the dominant reaction. Illumination of untreated, dark-adapted photosystem II membranes at 140 K or higher results in formation of the S_2 state of the Mn complex in samples limited to stabilizing a single charge separation per photosystem II center by DCMU (de Paula et al., 1985). At temperatures below 130 K the Mn complex is unable to donate electrons rapidly so the products of an alternate electron donation pathway are observed instead [see Scheme I and de Paula et al. (1985)]. In untreated photosystem II membranes, cytochrome b-559 is observed to be photooxidized, via Chl, by illumination at temperatures below 130 K (de Paula et al., 1985; Thompson & Brudvig, 1988). However, if cytochrome b-559 is chemically oxidized and, therefore, unable to reduce Chl$^+$, Chl$^+$ can be trapped (de Paula et al., 1985). These and other observations indicate that electron donation in photosystem II is dominated by three competing pathways of electron donation: from the Mn complex (and ultimately H_2O) via Y_Z; from cytochrome b-559 via Chl, possibly as part of a cyclical path of electron transport that protects against photoinhibition (Thompson & Brudvig, 1988); and from Y_D (Scheme I).

This detailed picture of electron donation in O_2-evolving photosystem II membranes offers a starting point for investigations of the electron donation events in photoactivation. The starting material for photoactivation experiments is NH_2OH-treated photosystem II membranes, in which the Mn complex has been removed. Many of the strategies that have been used to characterize the electron donation reactions in O_2-evolving photosystem II membranes are also applicable to NH_2OH-treated photosystem II membranes.

The experiments discussed in this paper were designed to identify the electron transport pathways that function in NH_2OH-treated photosystem II membranes and to determine how they contribute to photoactivation. By limiting electron transport to a single charge separation per photosystem II, we have obtained detailed information about the first step of photoactivation and examined the roles of various components

of photosystem II in photoactivation. Furthermore, we have obtained insight into the low yield of photoactivation in photosystem II membranes and are able to explain the low quantum yield of photoactivation.

EXPERIMENTAL PROCEDURES

Sample Preparation. All manipulations were performed in dim green light, on ice. Photosystem II membranes were prepared from spinach by using the method of Berthold et al. (1981) as modified by Beck et al. (1985) and resuspended in Ca buffer [20 mM MES/NaOH, pH 6.0, 15 mM $CaCl_2$, and 30% (v/v) ethylene glycol] for storage at 77 K. Untreated photosystem II membranes were treated with 5 mM NH_2OH to remove Mn as in Tamura and Cheniae (1987a) in buffer A (50 mM MES/NaOH, pH 6.5, 15 mM NaCl, 1 mM $CaCl_2$, and 0.4 M sucrose). The NH_2OH-treated photosystem II membranes were stored at 77 K in buffer A or in a buffer composed of 25 MES/NaOH, pH 6.5, 10 mM NaCl, and 30% (v/v) ethylene glycol. The untreated photosystem II membranes typically had O_2-evolution activities of 450–600 μmol of O_2/(mg of Chl·h) and an average of 204 Chl/4 Mn [$\sigma = 9$, five independent determinations of Mn^{2+} released by hydrolysis in HCl, as in Yocum et al. (1981)]. The Chl concentration was assayed by the method of Arnon (1949), and O_2-evolution activity was assayed as in Beck et al. (1985). The NH_2OH-treated photosystem II membranes had residual O_2-evolution activities of up to 30 μmol of O_2/(mg of Chl·h) and retained 0.1–0.3 Mn/200 Chl on the basis of Mn released by hydrolysis in HCl. Less than 5% of the extrinsic 33-kDa polypeptide, 25% of the extrinsic 23-kDa polypeptide, and 40% of the extrinsic 17-kDa polypeptide were lost in the NH_2OH treatment, as determined by SDS–PAGE and staining with Coomassie brilliant blue [as in de Paula et al. (1986)].

In some experiments, the extrinsic 17- and 23-kDa polypeptides were removed as well as Mn. This was accomplished by treatment with 0.8 M Tris at pH 8.2 (Yocum et al., 1981); 0.1–0.6 Mn/200 Chl, no detectable 17- or 23-kDa polypeptide, and less than 30% of the 33-kDa polypeptide remained after this treatment on the basis of Mn released by HCl hydrolysis and SDS–PAGE.

Spectroscopic Measurements. EPR samples consisted of NH_2OH-treated photosystem II membranes washed twice by resuspension to 0.2–0.5 mg of Chl/mL in the buffer to be used [20 mM MES/NaOH, pH 6.5, 50 mM $CaCl_2$ and 30% (v/v) ethylene glycol unless specified otherwise] followed by centrifugation for 10 min at 37000g. The (NH_2OH-treated) photosystem II membranes were then resuspended to 4–8 mg of Chl/mL. DCBQ was used to oxidize cytochrome b-559, and DCMU was used to restrict each photosystem II center to a single charge separation. When these were included, 25 mM DCBQ in ethanol and/or 5 mM DCMU in ethanol were added to photosystem II membranes to give final concentrations of 0.5 and 0.1 mM, respectively, unless specified otherwise. When Mn^{2+} was supplied, 10 mM $MnSO_4$ in water was added to give a final concentration of 0.2 mM, unless specified otherwise.

EPR signals from photosystem II were observed and quantitated as in de Paula et al. (1985). A sample of untreated photosystem II membranes illuminated for 1–2 min at 273 K, frozen immediately, and observed within a couple of hours contains Y_D^+, but no Chl$^+$, in all photosystem II centers, and was used as a spin standard for one free-radical spin per photosystem II center on the basis of integrated signal areas. A sample of untreated photosystem II membranes treated with 2 mM K_2IrCl_6 was used as a spin standard for two oxidized cytochromes b-559 per photosystem II center on the basis of

the integrated area of the g_z turning point (de Paula et al., 1985).

Mn^{2+} was quantitated by EPR using the amplitudes of the four outermost lines of the $Mn^{2+}(H_2O)_6$ signal as a measure of the Mn^{2+} concentration. Mn^{2+} quantitations by this method can be complicated by the fact that Mn^{2+} bound asymmetrically can give an identical signal only one-fourth as large as the signal from symmetrically coordinated Mn^{2+}. In addition, if the zero-field splitting of Mn^{2+} is large, the EPR signal will be broadened and difficult to detect. Nonetheless, essentially all of the Mn^{2+} added to photosystem II membranes in buffers containing ≥ 1 mM Ca^{2+} produced an EPR signal with the full possible amplitude on the basis of the following observations. The signal from Mn^{2+} added to photosystem II membranes was found to have the same intensity as that of an equal concentration of Mn^{2+} in buffer. Moreover, Mn^{2+} was visible in photosystem II samples containing only 0.3 Mn per photosystem II center without added Mn^{2+}, and the amplitude of the Mn^{2+} signal increased linearly with added Mn^{2+} up to a final concentration of 0.4 mM (26 μM photosystem II). Nonetheless, as a precaution, 50 mM $CaCl_2$ containing buffers were used to displace bound Mn^{2+} for the experiments in which quantitation of Mn^{2+} was important to the conclusions.

Mn^{2+} standards consisted of 10 mM $MnSO_4$ diluted to 0.2 mM in the same buffer as was used for the photosystem II samples, unless specified otherwise. The accuracy of Mn quantitations was limited to approximately 10 μM or approximately 0.3 Mn^{2+} per photosystem II center.

EPR samples were illuminated in a N_2 flow system after several minutes of equilibration in darkness at the chosen temperature and then immediately frozen in liquid N_2, as in de Paula et al. (1985), except when the illumination temperature was to be 273 K. In that case a (transparent) Dewar filled with ice and water was used for the illumination, and the samples were wiped dry quickly before freezing in liquid N_2. Cooling to 77 from 273 K took 20 s from the time the light was turned off.

RESULTS

Electron Transport in NH_2OH-Treated Photosystem II Membranes. To determine which electron carriers are photochemically active in Mn-depleted photosystem II, the results of illuminating NH_2OH-treated and untreated photosystem II membranes were compared. In these experiments, samples were illuminated with continuous light in the presence of DCMU until a stable charge separation was produced. EPR spectroscopy was then used to determine which electron donors and acceptors gave rise to the stable charge separation. The yields of photooxidation of the various electron donors reflect the relative rates of electron donation by each donor. Unstable charge-separated states, such as $Y_Z^+Q_A^-$ and $P680^+Q_A^-$, are not directly detected because they recombine before the EPR measurements are made. These unstable charge-separated states may repeatedly form and recombine during the continuous illumination until a stable charge separation occurs. Previous studies on untreated samples (de Paula et al., 1985; Thompson & Brudvig, 1988) have led to the scheme for electron donation shown in Scheme I. Because electron donation from cytochrome *b*-559 and Y_D competes with electron donation from the Mn complex in untreated photosystem II, one would expect electron donation from Y_D and cytochrome *b*-559 to gain importance in the absence of the Mn complex. This is especially true because treatment with NH_2OH does not induce oxidation of cytochrome *b*-559 (by converting it to the low-potential form) as do other treatments to remove Mn (Thompson et al., 1989), and NH_2OH also reduces Y_D^+,

Table I: Fractional Charge Stabilized by Each of the Various Electron Carriers of Photosystem II upon Illumination at 215 K, in NH_2OH-Treated and Untreated Photosystem II Membranes[a]

| | electron carrier | | | |
sample	cytochrome *b*-559	Mn complex[b]	Y_D + Chl	Q_A[c]
NH_2OH	0.54	0.07	0.37	0.70
untreated	0	0.74	0.26	1.0

[a] The photosystem II membranes were limited to approximately one stable charge separation per photosystem II center by 0.1 mM DCMU. The untreated photosystem II membranes were suspended in Ca buffer (see Experimental Procedures), and the NH_2OH-treated photosystem II membranes were suspended in 25 mM MES/NaOH, pH 6.5, 15 mM $CaCl_2$, 200 mM NaCl, and 30% ethylene glycol. Samples were illuminated at 215 K for 5 min. EPR conditions except for Y_D + Chl: microwave frequency, 9.1 GHz; temperature, 7 K; microwave power, 0.4 mW; field modulation amplitude, 20 G; field modulation frequency, 100 kHz. EPR conditions for Y_D + Chl: as in Figure 1A but with microwave power of 0.13 mW. [b] The amount of the S_2-state Mn complex formed in the untreated photosystem II membranes was calculated by assuming that the sum of all oxidized electron donors in untreated photosystem II membranes was equal to 1 (de Paula et al., 1985) and subtracting the observed amounts of Y_D^+, Chl^+, and cytochrome *b*-559 formed. This value was then used to calculate the amount of the S_2-state Mn complex formed in the NH_2OH-treated photosystem II membranes on the basis of the relative amplitudes of the four strongest lines in the high-field half of the S_2-sate multiline EPR signal. [c] The amount of $Fe^{2+}Q_A^-$ formed per untreated photosystem II center was assumed to be 1 (de Paula et al., 1985), and the amount of $Fe^{2+}Q_A^-$ formed in NH_2OH-treated photosystem II membranes was calculated on the basis of the relative signal amplitudes.

normally present in about 75% of photosystem II centers.

Upon illumination at 215 K, one does observe photooxidation of Y_D and cytochrome *b*-559 in NH_2OH-treated photosystem II membranes, in lieu of photooxidation of the Mn complex (Table I). Therefore, electron transport in NH_2OH-treated photosystem II follows the pattern expected on the basis of electron transport in untreated photosystem II (Scheme I). The less than quantitative amount of Q_A^- formed in NH_2OH-treated photosystem II membranes can be ascribed to the presence of $Fe^{3+}Q_A$ in some NH_2OH-treated photosystem II centers prior to illumination, on the basis of detection of the EPR signal from that species. Nonetheless, the sum of photooxidized electron donors is approximately one per photosystem II in NH_2OH-treated photosystem II membranes, indicating that all the redox-active components that stabilize charge separations in untreated photosystem II membranes retain the ability to do so in NH_2OH-treated photosystem II membranes, except of course the Mn complex which is absent. Thus, the electron donation pathways observed in O_2-evolving photosystem II membranes (Scheme I) can be used as the basis for understanding electron transport in NH_2OH-treated photosystem II membranes leading to Mn photoligation.

As shown in Table I, cytochrome *b*-559 is photooxidized in over half of the NH_2OH-treated photosystem II centers. To photooxidize other electron donors in high yield, it is necessary to prevent photooxidation of cytochrome *b*-559 by chemically oxidizing it prior to illumination. Then, by determining which electron donors are photooxidized in photosystem II over a range of temperatures, one can obtain insight into the relationships between the remaining electron donation alternatives.

In this experiment, the method used to ensure oxidation of cytochrome *b*-559 was depletion of the extrinsic polypeptides (and Mn) by treatment with Tris. Effects due to the absence of the Mn complex may be identified by comparing the behavior of these polypeptide- and Mn-depleted photosystem II membranes with that of 1 M $CaCl_2$ treated photosystem II membranes, which also lack the extrinsic polypeptides but
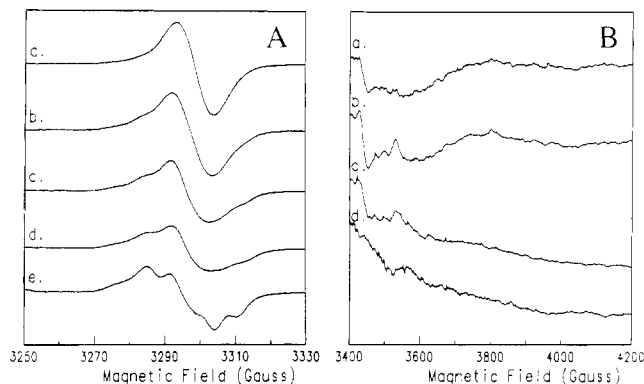
FIGURE 1: EPR signals of species trapped after illumination of NH_2OH-treated photosystem II membranes at a range of temperatures. The spectra shown are illuminated-minus-dark difference spectra obtained from 2-min illuminations at (a) 207 K and (b) 218 K or from 1-min illuminations at (c) 232 K and (d) 242 K. (e panel A only) A spectrum of Y_D^+, shown for comparison, was generated by illumination of untreated photosystem II membranes for 1 min at 273 K. NH_2OH-treated photosystem II membranes were suspended in buffer A, containing 0.25 mM DCBQ and 0.1 mM $MnCl_2$. (Panel A) Free-radical signals observed at 100 K with 0.2-mW microwave power, 4-G magnetic field modulation amplitude, 9.1-GHz microwave frequency, and 100-kHz magnetic field modulation frequency. (Panel B) $Fe^{2+}Q_A^-$ observed at 4 K with 22-mW microwave power, 20-G magnetic field modulation amplitude, 9.1-GHz microwave frequency, and 100-kHz magnetic field modulation frequency.

retain the Mn complex (Miller et al., 1987). Although illumination of the two types of sample produced the same results at 77 and 140 K, at 210 and 273 K, temperatures at which the Mn complex is normally the dominant electron donor and charge separation is stabilized at all photosystem II centers, only 50% and 20% of Mn-depleted photosystem II centers stabilized a charge separation, respectively (data not shown). Because it is extremely unlikely that no charge separation occurred in the other 50% and 80% of sites, respectively, we interpret this result as evidence for photooxidation of a species that recombines with Q_A^- after illumination. This species cannot be Chl, because Chl$^+$ can be trapped after illumination at 210 K (Miller et al., 1987). Instead, the analogy between electron donation in the presence and absence of the Mn complex suggests that the untrapped species is Y_Z^+. Indeed, the analogy is strengthened by optical measurements on NH_2OH-treated photosystem II membranes which indicate that the initial product of charge separation is $Y_Z^+Q_A^-$ (Buser et al., 1990). One way to further test the hypothesis that Y_Z is being photooxidized in addition to cytochrome b-559, Chl, and Y_D is to provide an extrinsic electron donor that is thought to be oxidized by Y_Z^+ but which is stable enough when oxidized to be trapped as evidence for the photooxidation of Y_Z. Although it may not be oxidized every time Y_Z^+ is formed, Mn^{2+} is such an electron donor (Hoganson et al., 1988) and can serve as an indicator of photooxidation of Y_Z.

Electron Transport in NH_2OH-Treated Photosystem II Membranes with Added Manganese. Because photoactivation necessarily involves more than one charge separation (Cheniae & Martin, 1971) and also involves photooxidation of Mn^{2+} (Tamura & Cheniae, 1989), we have extended our characterization of electron donation in Mn-depleted photosystem II to a study of electron donation in the presence of Mn^{2+}, with the possibility of multiple turnovers. DCBQ was added to oxidize cytochrome b-559 and prevent it from donating an electron. DCMU was not used, so that at temperatures above 230 K DCBQ is expected to reoxidize photoreduced Q_A^- and allow more than one charge separation to be stabilized by each photosystem II (Beck et al., 1985). The effects of illumination

Table II: Products of Charge Separation in NH_2OH-Treated Photosystem II Membranes, at Illumination Temperatures Ranging from 210 to 240 K[a]

temp of illumination (K)	Chl + Y_D[b]	Mn[b]	$\sum_D$[c]	Q_A[d]
207	0.9	0	0.9	1.0
218	1.0	0	1.0	0.9
232	0.8	0.3	1.1	0.4
242	0.8	0.2	1.0	0.2

[a] All conditions were as in Figure 1. [b] Yields of photooxidized Y_D and Chl, and silenced Mn^{2+}, are given in stoichiometric equivalents to photosystem II centers. [c] $\sum_D$ is the total extent of electron donor photooxidation, here equal to Chl + Y_D + Mn. [d] The amount of $Fe^{2+}Q_A^-$ formed at 207 K was assumed to be 1 and the amounts of $Fe^{2+}Q_A^-$ formed at other temperatures are calculated from that on the basis of the relative signal amplitudes.
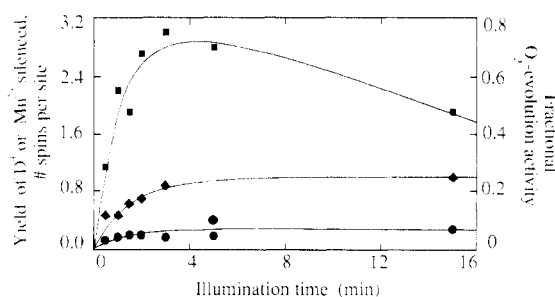

FIGURE 2: Time course of Mn^{2+} photooxidation, photooxidation of Y_D, and photoactivation in the course of illumination of EPR samples at 273 K. (■) Mn^{2+} silenced; (◆) photooxidation of Y_D; (●) yield of photoactivation. NH_2OH-treated photosystem II membranes were suspended in buffer A with 5 mM Ca^{2+}, 100 mM Cl$^-$, 340 μM Mn^{2+}, and 0.86 mM DCBQ (8 Mn^{2+} and 20 DCBQ per photosystem II). Mn^{2+} silenced with respect to EPR and Y_D photooxidized are in stoichiometric ratios to photosystem II centers, as calculated from EPR signal amplitudes (left axis) (EPR conditions as in Table I). The fractional O_2-evolution activity is the activity measured after the EPR experiment and is expressed as a fraction of the O_2-evolution activity of untreated photosystem II membranes, on a scale 4 times as large as the left-hand scale, to reflect the fact that 4 Mn must be incorporated to reconstitute O_2-evolution activity.

at temperatures ranging from 210 to 240 K were compared because our previous experiment indicated that Y_Z^+ is present during illumination at and above 210 K, and the expected onset temperature of multiple turnovers is approximately 230 K.

Figure 1 displays the trends observed following illumination at increasing temperatures from 210 to 240 K. In this temperature range we observe a correlation between the decrease in the EPR signal due to Mn^{2+}, the increasing contribution of Y_D to electron donation, and the decrease in the amounts of Chl$^+$ and FeQ$_A^-$ trapped. Decreasing amounts of trapped Chl$^+$ can be explained by the decreased stability of Chl$^+$ at higher temperatures, probably due to recombination. However, the fact that the decrease in the yield of trapped FeQ$_A^-$ is accompanied by an increase in the total yield of oxidized electron donors indicates that Q_A^- is reoxidized by DCBQ in some centers. The magnitudes of these effects are given in Table II.

The photooxidation of Y_D and the decrease in the EPR signal from Mn^{2+} are also correlated in time with the acquisition of O_2-evolution activity, as shown in Figure 2. Although the magnitudes of these effects differ by up to an order of magnitude, their time courses are the same. Photooxidation of Mn^{2+} in excess of the amount of Mn photoligated is consistent with reports of Mn^{2+} photooxidation not leading to restoration of O_2-evolution activity (Klimov et al., 1982) and our measurements of silencing of the EPR signal from more than 4 Mn^{2+} per photosystem II center in experiments

Table III: Electron Donors Photooxidized in NH_2OH-Treated Photosystem II Centers Limited to One Stable Charge Separation[a]

temp of illumination (K)	Mn^b	$Chl + Y_D^b$
240	0.8	0.2
230	0.6	0.25

[a] NH_2OH-treated photosystem II membranes contained 0.1 mM DCMU and 0.2 mM Mn^{2+}; the DCBQ used to oxidize cytochrome b-559 was washed out to less than 0.05 mM. [b] Mn^{2+} silenced or yield of Y_D^+, in stoichiometric equivalents to photosystem II. EPR instrumental conditions as in Figure 3 for Chl^+ and Y_D^+, and the same for Mn^{2+} except magnetic field modulation amplitude, 20 G, and temperature, 7 K.

with higher added Mn^{2+} concentrations (not shown). The reappearance of an EPR signal from Mn^{2+} at long illumination times may be due to accumulation of reduced DCBQ, photoreduced by photosystem II, which would reduce EPR-silent Mn^{3+} back to EPR-visible Mn^{2+}. We conclude that the silencing of Mn^{2+} observed in the EPR experiments reflects the Mn^{2+} photooxidation involved in photoactivation, although it exceeds the amount of Mn functionally photoligated.

Together, the data in Table II and Figures 1 and 2 show correlations between photoactivation and recombination of $Chl^+Q_A^-$, photooxidation of Y_D, multiple turnovers, and silencing of the Mn^{2+} EPR signal. However, the possibility remains that the decrease in the EPR signal from Mn^{2+} is due to a change in the coordination geometry of Mn^{2+}, instead of photooxidation. In the experiments that follow, we have quantitated the electron donors that are photooxidized in samples restricted to a single, stable charge separation. This has enabled us to determine whether the decrease in amplitude of the Mn^{2+} EPR signal is due to photooxidation of Mn^{2+}. From these experiments, we have also determined whether photooxidation of cytochrome b-559, Chl, or Y_D, all of which occur during photoactivation, is necessary for photoactivation or simply reflects alternate electron donation reactions that occur in competition with the reactions leading to photoactivation.

Single-Electron-Transfer Events. In the experiments discussed in this section, and the sections that follow, DCMU was added to all samples to restrict each photosystem II center to stabilizing approximately one charge separation. The total extent of electron donor photooxidation was calculated in each case, as a measure of the number of charge separations stabilized per photosystem II center. Furthermore, samples were prepared in 50 mM $CaCl_2$ containing buffer to ensure that all of the Mn^{2+} was visible by EPR.

In the first experiment, photochemistry was limited to stable photooxidation of Y_D or Mn^{2+} by first chemically oxidizing cytochrome b-559 and then illuminating at 230 or 240 K, temperatures at which Y_Z^+ and Chl^+ recombine with Q_A^-. The number of oxidation equivalents accounted for by silencing of the Mn^{2+} EPR signal and oxidation of other electron donors (Y_D and some Chl) was approximately 1 per photosystem II center, as expected for DCMU-treated samples (Table III). Therefore, we conclude that the only process silencing the EPR signal from Mn^{2+} in these experiments is photooxidation of Mn^{2+} to Mn^{3+} and that photooxidation of Mn^{2+} does not depend on the occurrence of multiple charge separations.

The coincident increases in photooxidation of Y_D and Mn^{2+} and recombination of $Chl^+ Q_A^-$ observed after shorter illuminations, at a range of temperatures (Figure 1), could indicate that Y_D^+ and Mn^{3+} are produced in competition with photooxidation of Chl. Although low-temperature illuminations indicate that Chl is stably photooxidized in NH_2OH-treated photosystem II centers, rapid recombination of Chl^+
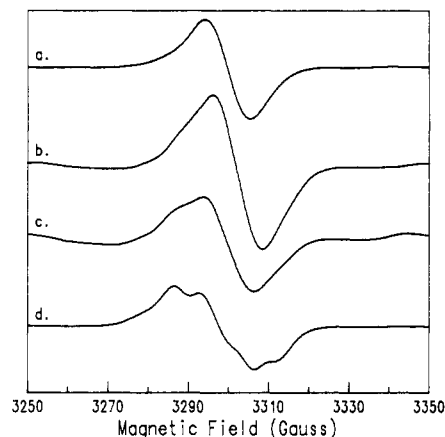

FIGURE 3: Time course of illumination at 215 K of NH_2OH-treated photosystem II membranes limited to a single stable charge separation per center (by 0.1 mM DCMU), with cytochrome b-559 chemically oxidized (by using 0.5 mM DCBQ) and with 0.2 mM Mn^{2+} added. Illuminated-minus-dark difference spectra are shown of (a) Chl^+ produced by illumination at 210 K, for comparison with the results of (b) 20-min illumination at 213 K, (c) 60-min illumination at 218 K, and (d) Y_D^+ produced by illuminating untreated photosystem II membranes at 273 K, also for comparison. (a) and (d) are shown at half the amplitude of (b) and (c) when scaled to the same Chl concentration. EPR instrumental conditions: microwave frequency, 9.1 GHz; temperature, 100 K; microwave power, 0.4 mW; magnetic field modulation amplitude, 4 G; magnetic field modulation frequency, 100 kHz.

and Y_Z^+ with Q_A^- at higher temperatures should result in each photosystem II center undergoing repeated charge separation-recombination cycles, providing each of the competing electron donors with several opportunities to donate an electron. No matter how low their quantum yields of photooxidation, competing electron donors giving more stable charge-separated states should make up an increasing fraction of the oxidized donors trapped as the illumination is extended. The stable products of photooxidation should be observed to replace the kinetic products in the course illumination, on a time scale much longer than that of the photooxidative events themselves.

Slow accumulation of the more stable products of photooxidation is, indeed, observed (Figure 3). Although 30 s of illumination is more than sufficient for a charge separation to occur at all photosystem II centers at 200 K, and no more than one charge separation was stabilized per photosystem II, the extent of photooxidation of Y_D and Mn^{2+} (evident as the increased rolls in the base line in Figure 3b,c) increased significantly over a period of 40 min at 215 K. Furthermore, similar trends were observed at 230 and 240 K on shorter time scales. Therefore, we conclude that an increasing rate of $Chl^+Q_A^-$ recombination with increasing temperature is responsible for the observed coincident increases with temperature of illumination of the yields of photooxidation of Mn^{2+} and Y_D (Figures 1 and 2 and Table II).

The above results support the view that substantial yields of Mn^{2+} photooxidation, such as those in Table III, are the result of numerous charge separations at each photosystem II center, all but the last of which generate Y_Z^+ or Chl^+ and, thus, are not stable. Furthermore, the above result can also explain the quantum yield for Mn^{2+} photooxidation in photoactivation of only 1% (Cheniae & Martin, 1971) as the result of slow Mn^{2+} photooxidation, relative to photooxidation of Y_Z and Chl.

Role of Y_D in Photooxidation of Manganese. The data we have presented so far do not discriminate between the possibilities that Mn^{2+} photooxidation is mediated by Y_D or that Mn^{2+} and Y_D compete to reduce the same species (Y_Z). To

Table IV: Competition between Photooxidation of Y_D and Photooxidation of Mn^{2+} [a]

	photooxidation of Y_D [b]	photooxidation of Mn^{2+} [b]
no Mn^{2+}	0.5	
0.2 mM Mn^{2+}	0.3	1.0

[a] NH_2OH-treated photosystem II membranes contained 0.1 mM DCMU to limit each center to stabilizing only one charge separation; the DCBQ used to oxidize cytochrome b-559 was washed out to less than 0.05 mM. Illumination was at 240 K for 10 min. [b] Y_D and Mn^{2+} photooxidized, in stoichiometric equivalents to photosystem II. Y_D, EPR conditions as in Figure 3; Mn^{2+}, EPR conditions as in Table I except microwave power, 1.3 mW.

determine whether Y_D^+ could, in turn, oxidize Mn^{2+}, Y_D^+ was produced by illumination in a pair of samples (containing 0.1 mM DCMU and less than 0.05 mM residual DCBQ). Mn^{2+} was added to one sample immediately after illumination (0.2 mM final concentration). In the course of 10 min of incubation at 273 K in the dark neither sample displayed significant reduction of Y_D^+, nor was Mn^{2+} oxidized in the sample to which it had been added. By contrast, in a third similar sample that contained 0.2 mM Mn^{2+} prior to illumination, 1 min of illumination at 273 K led to Mn^{2+} photooxidation equivalent to 1 Mn per photosystem II center. Therefore, significant Mn^{2+} oxidation is expected in the course of a 10-min incubation if Y_D^+ oxidizes Mn^{2+}, and the fact that this was not observed indicates that photooxidation of Mn^{2+} is not mediated by Y_D in the first step of photoactivation.

If the photooxidations of Y_D and Mn^{2+} are two independent processes, they are expected to compete with one another. This is indeed observed, as demonstrated in Table IV. Illumination of a sample of NH_2OH-treated photosystem II membranes with added Mn^{2+} produced only about half as much Y_D^+ as illumination of a similar sample without Mn^{2+}, in a single charge separation. Therefore, we conclude that electron donation from Y_D and electron donation from Mn^{2+} are two independent, competing processes.

Role of Cytochrome b-559 in Photooxidation of Manganese. NH_2OH-treated photosystem II membranes retain most of their extrinsic polypeptides, and cytochrome b-559 is mostly reduced in the dark, photochemically active, and thus potentially important in photoactivation. However, throughout all but the first experiment described (Table I), cytochrome b-559 was chemically oxidized so that the photooxidation of other electron donors could be studied instead. However, if cytochrome b-559 were capable of oxidizing Mn^{2+}, then one would expect that when Mn^{2+} was added to NH_2OH-treated photosystem II membranes in the presence of DCBQ, which chemically oxidizes cytochrome b-559, a fraction of the Mn^{2+} would be oxidized. This was not observed. Therefore, and because cytochrome b-559 can be photooxidized in the absence of Mn^{2+}, we conclude that cytochrome b-559 and Mn^{2+} are photooxidized independently of one another, as are cytochrome b-559 and the Mn complex in untreated photosystem II membranes. Thus, cytochrome b-559 does not play a direct role in Mn^{2+} photooxidation in the first step of photoactivation.

DISCUSSION

Electron Transport and Photooxidation of Mn^{2+} in Mn-Depleted Photosystem II. We have used EPR to study the electron-transfer reactions of photosystem II membranes treated with NH_2OH to remove the Mn complex. These experiments show that photooxidation of added Mn^{2+} occurs in competition with photooxidation of Y_D, Chl, and cytochrome b-559. This is consistent with Mn^{2+} being photooxidized via

Y_Z, as is the native Mn complex. Indeed, electron transport in NH_2OH-treated photosystem II membranes was found to be identical with electron transport in untreated photosystem II membranes, except that S-state advancement is replaced by slower electron donation from exogenous Mn^{2+}.

Our results show that the first photooxidative event in photoactivation results in oxidation of one Mn^{2+} to Mn^{3+}, and cytochrome b-559, Chl, and Y_D have been excluded from playing roles in the first photooxidative event of photoactivation. These results provide direct evidence that the species photooxidized in the first step of photoactivation is Mn^{2+}, as has been proposed by Tamura and Cheniae (1989).

Although photoactivation is known to require two photooxidative events (Ananyev et al., 1988; Ono & Inoue, 1987), we have worked primarily with photosystem II membranes limited to stabilizing a single charge separation. Thus, our results apply to the first step of photoactivation. However, the similarity between electron transport in untreated samples containing an assembled Mn complex and electron transport in Mn-depleted samples with exogenous Mn^{2+} as an electron donor instead indicates that the electron donation pathways in photosystem II do not change during photoactivation. Rather, it is the relative rates of the various electron donation reactions that change as a functional Mn complex is assembled. Therefore, our results suggest that the second photochemical step of photoactivation is like the first and consists of photooxidation of Mn^{2+} in competition with Y_D, Chl, and cytochrome b-559. Thus, we conclude that cytochrome b-559, Y_D, and Chl are not directly involved in the photochemistry of photoactivation. This conclusion (and the associated similarity between electron transport in the first and second photochemical steps of photoactivation) is further supported by the fact that removal of Y_D by site-directed mutagenesis does not prevent assembly of the Mn complex (Debus et al., 1988) nor does conversion of cytochrome b-559 to its low-potential form by depletion of the extrinsic polypeptides (Tamura & Cheniae, 1986).

Mn^{2+} is photooxidized to a significant extent only after multiple cycles of charge separation and recombination at temperatures of 215 K or above. This indicates that electron donation from Mn^{2+} is slower than electron donation from Chl and recombination of $Y_Z^+Q_A^-$. The high Ca^{2+} concentrations we have employed to ensure that all Mn^{2+} is visible by EPR may slow electron donation from Mn^{2+} somewhat by limiting the access of Mn^{2+} to its binding site. However, the Ca^{2+} and Mn^{2+} concentrations we have used (50 mM Ca^{2+}, 0.2 mM Mn^{2+}) are close to concentrations that produce optimal photoactivation yields (40% in 50 mM Ca^{2+}, 0.6 mM Mn^{2+}) in similar NH_2OH-treated photosystem II membranes (Miller & Brudvig, 1989). Therefore, our EPR results reflect events that occur in the course of efficient photoactivation. Furthermore, the relatively slow electron donation from Mn^{2+} we observe in competition with photooxidation of Chl and recombination of $Y_Z^+Q_A^-$ offers an explanation for the low quantum yield of photoactivation.

Slow electron donation from Mn^{2+} relative to electron donation from Chl could also be responsible for the low yield of photoactivation because Chl photooxidation is postulated to precede photoinhibition (Thompson & Brudvig, 1988). Although intact chloroplasts can compensate for this by repairing photoinhibited photosystem II centers (Callahan et al., 1986), photoinhibition lowers the yield of photoactivation that can be obtained from isolated photosystem II membranes.

Mechanism of Photoactivation. Our quantitative studies of Mn^{2+} photooxidation provide information on the interme-

diates involved in Mn photoligation and insight into the mechanism of photoactivation [see Miller and Brudvig (1989) and Tamura and Cheniae (1987a)]. Photoactivation involves two light-dependent steps separated by a light-independent step (Cheniae & Martin, 1971; Ono & Inoue, 1987), and two photochemical events suffice to produce a stable intermediate that spontaneously completes photoactivation (Ananyev et al., 1988; Ono & Inoue, 1987).

The Mn ions in the active Mn complex are in an oxidation state higher than Mn^{2+}, and conditions that decrease net Mn^{2+} photooxidation also reduce the yield of photoactivation (Tamura & Cheniae, 1989). Therefore, photooxidation of Mn^{2+} is believed to be an important component of Mn photoligation. The correlated time courses of Mn^{2+} photooxidation and photoactivation we observe confirm this. Furthermore, the EPR signal of only one Mn^{2+} is silenced upon formation of the first intermediate, indicating that one Mn^{2+} is oxidized to Mn^{3+} independent of other Mn^{2+} ions.

Mn^{2+} can also be spontaneously oxidized to Mn^{3+} when its coordination decreases its reduction potential sufficiently to allow autoxidation to occur in the presence of O_2, as in the case of Mn superoxide dismutase (Brock & Walker, 1980). However, autoxidation of Mn^{2+} upon coordination is ruled out in the first step of photoactivation by our observation that all added Mn is visible by EPR as Mn^{2+}, under conditions that, nonetheless, favor photoactivation. Therefore, we conclude that the first photochemical event of photoactivation results in formation of an intermediate of Mn complex assembly consisting of only one Mn^{3+} ion.

Studies of the Mn^{2+} and Ca^{2+} dependence of the rate and yield of photoactivation indicated that a single Mn^{2+} ion is reversibly bound prior to the rate-determining steps of Mn photoligation (Miller & Brudvig, 1989). The different magnitudes of the dissociation constants for Mn reported for photoactivation (Miller & Brudvig, 1989; Ono & Inoue, 1983) or in connection with simple Mn^{2+} photooxidation (Hsu et al., 1987; Klimov et al., 1982) and kinetic considerations suggest that the first-order Mn^{2+} concentration dependence of photoactivation reflects Mn^{2+} binding in preparation for the second photochemical event in Mn photoligation (Miller & Brudvig, 1989). Thus, an intermediate containing $Mn^{3+}Mn^{2+}$ is indicated. On the basis of the similarity of the electron donation reactions in untreated and Mn-depleted samples, we argue that the second photochemical step of photoactivation results in photooxidation of Mn^{2+} as does the first. Thus, the intermediate of Mn complex assembly generated by two photochemical events, the first intermediate that completes photoactivation instead of backreacting (Ananyev et al., 1988; Ono & Inoue, 1987), is expected to contain Mn^{3+}_2. Such an intermediate has been postulated on the basis of the results of partial depletion of Mn from photosystem II (Tamura & Cheniae, 1987a).

We cannot rule out spontaneous oxidation of the two final Mn ions that must bind to complete assembly of the Mn complex. However, inhibition of photoactivation in flashing light by reductants can be counteracted by increasing the flash frequency (Tamura & Cheniae, 1987b). This suggests that the intermediates involved in the two photochemical steps are more sensitive to reductants than the events that follow. Thus, it is simplest to assume that the third and fourth Mn ions are bound as Mn^{2+} and, therefore, that the first tetrameric intermediate of Mn complex assembly consists of $Mn^{3+}_2Mn^{2+}_2$.

The most reduced stable tetrameric state of the Mn complex is the S_{-1} state, which is formed upon treatment of photosystem II with dilute NH_2OH (Beck & Brudvig, 1987). Equating

the S_{-1} state with the least oxidized tetrameric state of the Mn complex, described above, leads to identification of the S_2 state of the Mn complex as $Mn^{4+}Mn^{3+}_3$. This assignment is one of two possibilities that have been considered widely and is consistent with available spectroscopic data on the S_2 state of the Mn complex and information on the mechanism of O_2 evolution [reviewed in Brudvig and Crabtree (1989)].

The mechanism of Mn complex assembly is suggestive of the type of amino acid side chains involved in ligating Mn to photosystem II. In most of the enzymes in which Mn is present as Mn^{2+}, Mn^{2+} is ligated primarily via O from carboxylate, phosphate, or hydroxy groups [reviewed in McEuen (1982) and Markham (1986)]. By contrast, in the enzymes that contain Mn^{3+}, for which information is available, ligation is primarily via N and/or S (Ludwig et al., 1986; Sugiura et al., 1980, 1981). These observations are consistent with the greater ability of N and S coordination to stabilize higher formal oxidation states of bound Mn. Stabilization by N ligands causes Mn to be autoxidized to Mn^{3+} upon ligation to superoxide dismutase (Brock & Walter, 1980) and necessitates addition of dithionite to generate the Mn^{2+} state of Mn-substituted porphyrins in hemoglobin (Yonetani et al., 1970) and myoglobin (Hori et al., 1984). By contrast, photochemically driven oxidation is necessary for incorporation of Mn into photosystem II. This distinction indicates that the reduction potential of Mn^{2+}/Mn^{3+} in photosystem II is higher than in superoxide dismutase and presents new chemical evidence that Mn in photosystem II is ligated primarily via O instead of N.

REFERENCES

Ananyev, G. M., Shafiev, M. A., Isaenko, T. V., & Klimov, V. V. (1988) *Biofizika 33*, 265.

Arnon, D. I. (1949) *Plant Physiol. 24*, 1.

Babcock, G. T., & Sauer, K. (1975) *Biochim. Biophys. Acta 376*, 315.

Beck, W. F., & Brudvig, G. W. (1987) *Biochemistry 26*, 8285.

Beck, W. F., de Paula, J. C., & Brudvig, G. W. (1985) *Biochemistry 24*, 3035.

Berthold, D. A., Babcock, G. T., & Yocum, C. F. (1981) *FEBS Lett. 134*, 231.

Boussac, A., & Etienne, A. L. (1982) *Biochem. Biophys. Res. Commun. 109*, 1200.

Brock, C. J., & Walker, J. E. (1980) in *Chemical and Biochemical Aspects of Superoxide Dismutase* (Bannister, J. V., & Hill, H. A. O., Eds.) p 237, Elsevier/North-Holland, Amsterdam.

Brudvig, G. W., & Crabtree, R. H. (1989) *Prog. Inorg. Chem. 37*, 99.

Buser, C. A., Thompson, L. K., Diner, B. A., & Brudvig, G. W. (1990) *Biochemistry* (submitted for publication).

Callahan, F. E., Becker, D. W., & Cheniae, G. M. (1986) *Plant Physiol. 82*, 261.

Cheniae, G. M., & Martin, I. F. (1971) *Biochim. Biophys. Acta 253*, 167.

Cramer, W. A., Theg, S. M., & Widger, W. R. (1986) *Photosynth. Res. 10*, 393.

Debus, R. J., Barry, B. A., Babcock, G. T., & McIntosh, L. (1988) *Proc. Natl. Acad. Sci. U.S.A. 85*, 427.

de Paula, J. C., Innes, J. B., & Brudvig, G. W. (1985) *Biochemistry 25*, 6487.

de Paula, J. C., Li, P. M., Miller, A.-F., Wu, B. W., & Brudvig, G. W. (1986) *Biochemistry 25*, 6487.

Hoganson, C. W., Babcock, G. T., & Yocum, C. F. (1988) *Biophys. J. 53*, 616a.

Hori, H., Ikeda-Saito, M., Reed, G. H., & Yonetani, T. (1984) *J. Magn. Reson. 58*, 177.

Hsu, B. D., Lee, J. Y., & Pan, R.-L. (1987) *Biochim. Biophys. Acta 890*, 89.

Klimov, V. V., Allakhverdiev, S. I., Shuvalov, V. A., & Krasnovsky, A. A. (1982) *FEBS Lett. 148*, 307.

Ludwig, M. L., Pattridge, K. A., & Stallings, W. C. (1986) in *Manganese in Metabolism and Enzyme Function* (Schramm, V. L., & Wedler, F. C., Eds.) p 405, Academic Press, New York.

Markham, G. D. (1986) in *Manganese in Metabolism and Enzyme Function* (Schramm, V. L., & Wedler, F. C., Eds.) p 379, Academic Press, New York.

McEuen, A. R. (1982) *Inorg. Biochem. 3*, 314.

Miller, A.-F. (1989) Ph.D. Thesis, Yale University, New Haven, CT.

Miller, A.-F., & Brudvig, G. W. (1989) *Biochemistry 28*, 8181.

Miller, A.-F., de Paula, J. C., & Brudvig, G. W. (1987) *Photosynth. Res. 12*, 205.

Ono, T., & Inoue, Y. (1983) *Biochim. Biophys. Acta 723*, 191.

Ono, T.-A., & Inoue, Y. (1987) *Plant Cell Physiol. 28*, 1293.

Plesničar, M., & Bendal, D. S. (1973) *Biochem. J. 136*, 803.

Styring, S., & Rutherford, A. W. (1987) *Biochemistry 26*, 2401.

Sugiura, Y., Kawabe, H., & Tanaka, H. (1980) *J. Am. Chem. Soc. 102*, 6581.

Sugiura, Y., Kawabe, H., & Tanaka, H. (1981) *J. Am. Chem. Soc. 103*, 963.

Tamura, N., & Cheniae, G. M. (1986) *FEBS Lett. 200*, 231.

Tamura, N., & Cheniae, G. M. (1987a) *Biochim. Biophys. Acta 890*, 179.

Tamura, N., & Cheniae, G. M. (1987b) in *Progress in photosynthesis research* (Biggins, J., Ed.) Vol 1, p 621, Martinus Nijhoff, Dordrecht, The Netherlands.

Tamura, N., & Cheniae, G. M. (1989) in *Light Energy Transduction in Photosynthesis: Higher Plant and Bacterial Models* (Stevens, S. E., & Bryant, D. A., Eds.) p 227, American Soc. Plant Physiologists.

Thompson, L. K., & Brudvig, G. W. (1988) *Biochemistry 27*, 6653.

Thompson, L. K., Miller, A.-F., de Paula, J. C., & Brudvig, G. W. (1988) *Isr. J. Chem. 28*, 121.

Thompson, L. K., Miller, A.-F., Buser, C. A., de Paula, J. C., & Brudvig, G. W. (1989) *Biochemistry 28*, 8048.

Yocum, C. F., Yerkes, C. T., Blankenship, R. E., Sharp, R. R., & Babcock, G. T. (1981) *Proc. Natl. Acad. Sci. U.S.A. 78*, 7507.

Yonetani, T., Drott, H. R., Leigh, J. S., Jr., Reed, G. H., Waterman, M. R., & Asakura, T. (1970) *J. Biol. Chem. 245*, 2998.

Weak Binding of Divalent Cations to Plasma Gelsolin[†]

Yukio Doi,* Fimi Kim, and Shoko Kido

Department of Food Science, Kyoto Women's University, Higashiyama-ku, Kyoto 605, Japan

Received May 10, 1989; Revised Manuscript Received September 14, 1989

ABSTRACT: Calcium binding of swine plasma gelsolin was examined. When applied to ion-exchange chromatography, its elution volume was drastically altered depending on the free Ca^{2+} concentration of the medium. The presence of two classes of Ca^{2+} binding sites, high-affinity sites ($K_d = 7$ μM) and low-affinity sites ($K_d = 1$ mM), was suggested from the concentration dependence of the elution volume. The tight binding sites were specific for Ca^{2+}. The weakly bound Ca^{2+} could be replaced by Mg^{2+} once the tight binding sites were occupied with Ca^{2+}. The binding of metal ions was totally reversible. Circular dichroism measurement of plasma gelsolin indicated that most change in secondary structure was associated with Ca^{2+} binding to the high-affinity sites. Binding of Mg^{2+} to the low-affinity sites caused a secondary structural change different from that caused by Ca^{2+} bound to the high-affinity sites. Gel permeation chromatography exhibited a small change in Stokes radius with and without Ca^{2+}. Microheterogeneity revealed by isoelectric focusing did not relate to the presence of two classes of Ca^{2+} binding sites. These results indicated that plasma gelsolin drastically altered its surface charge property due to binding of Ca^{2+} or Ca^{2+}, Mg^{2+} with a concomitant conformational change.

Gelsolin is a calcium-dependent actin binding protein that nucleates actin filament growth, caps the fast-growing end of the filaments, and severs them (Coue & Korn, 1985, 1986; Doi & Frieden, 1984; Harris & Weeds, 1983; Pollard & Cooper, 1986; Janmey et al., 1985). It is found in a wide variety of vertebrate species both as an intrinsic cytoplasmic protein and as a secreted plasma protein (Yin et al., 1984). Cytoplasmic gelsolin first isolated from rabbit lung macrophages (Yin & Stossel, 1979) is a simple protein with a molecular weight of 83 000 (Kwiatkowski et al., 1986). Plasma gelsolin is structurally similar to cytoplasmic gelsolin except that it contains an additional residues at its NH_2 terminus, 25 and 9 amino acid residues, respectively, for human and pig plasma gelsolin (Kwiatokowski et al., 1986; Way & Weeds, 1988). Sequence analysis suggests that gelsolin belongs to a superfamily of the actin-severing proteins such as villin, severin, and fragmin (Andre et al., 1988).

Both gelsolins show Ca^{2+}-modulated interaction with G- and F-actin. Under nonpolymerizing conditions in the presence of Ca^{2+}, they form tight ternary complexes with two actin monomers (A_2G). Lowering the Ca^{2+} concentration with ethylene glycol bis(β-aminoethyl ether)-*N,N,N',N'*-tetraacetic acid (EGTA)[1] reduces the affinity for one actin, resulting in

---